Journal of Materials Chemistry A

RSC Publishing

PAPER

View Article Online
View Journal | View Issue

Defect chemistry and lithium-ion migration in polymorphs of the cathode material Li_2MnSiO_4†

Cite this: *J. Mater. Chem. A*, 2013, **1**, 4207

Craig A. J. Fisher,*[a] Navaratnarajah Kuganathan‡[b] and M. Saiful Islam[b]

The search for new low-cost and safe cathodes for next-generation lithium batteries has led to increasing interest in silicate materials. Here, a systematic comparison of crystal properties, defect chemistry and Li-ion migration behaviour of four polymorphs of Li_2MnSiO_4 is reported based on the results of atomistic simulations. The four polymorphs examined have $Pmn2_1$, $Pmnb$, $P2_1/n$, and Pn symmetry. Lattice energies of all four polymorphs are very similar, with only a small energy preference for the two orthorhombic phases over the monoclinic phases, which explains the difficulty experimentalists have had preparing pure-phase samples. Defect formation energies of the polymorphs are also similar, with antisite Li/Mn defects the most energetically favourable. Detailed analysis of the Li-ion migration energy surfaces reveals high activation energies (around 0.9 to 1.7 eV) and curved trajectories. All four polymorphs are thus expected to be poor Li-ion conductors, requiring synthesis as nanoparticles to facilitate sufficient Li transfer. The results accord well with experimental reports on the structure, relative phase stabilities and electrochemical performance of materials in this system.

Received 9th January 2013
Accepted 7th February 2013

DOI: 10.1039/c3ta00111c

www.rsc.org/MaterialsA

Introduction

The development of cheaper, safer and environmentally benign battery technologies, particularly for use in transport applications and large-scale storage of renewable energy, is one of the major challenges of the early 21st century.[1] Lithium-ion batteries have the highest energy densities of extant technologies, but their scale-up is hampered by problems associated with the most commonly used cathode material, $LiCoO_2$. Intensive research thus continues to be directed towards developing new cathode materials in order to expedite the move towards low-carbon technologies.

To date, several different materials systems have been investigated in the search for alternative cathode materials, including spinel-structured $Li(Mn_{1-x}M_x)_2O_4$ (M = Al, Fe, Co, Ni, Cr, *etc.*),[2,3] layer-structured Li_2MnO_3 (ref. 4) and solid solutions Li(Ni, Co, Mn)O_2,[5] olivine-type orthophosphates $LiMPO_4$ (M = Mn, Fe, Co, Ni),[6,7] and vanadophosphates such as $Li_3V_2(PO_4)_3$.[7–9] Recently, orthosilicates Li_2MSiO_4 (M = Fe, Mn, Co)[10–14] and their solid solutions[15] have also been found to display attractive electrochemical properties when used as cathode materials. Because their constituent elements are non-toxic, low-cost and abundant, they are also attractive systems from the standpoint of environmental sustainability.

A key feature of these silicates is that, in principle, extraction of two lithium ions is possible per formula unit, resulting in a two-electron process, with an average oxidation potential over 4 V. This should provide a higher capacity (theoretically about 330 mA h g^{-1} in the case of Li_2MnSiO_4) than the olivine phosphates, in which only one lithium ion can be extracted per formula unit. It has also been suggested that the second lithium can be more readily removed from Li_2MnSiO_4 than Li_2FeSiO_4 because the Mn^{4+} oxidation state is much more accessible than the Fe^{4+} oxidation state. To date, however, electrochemical studies have been unable to achieve such high capacities, with the serious capacity loss upon cycling being attributed to the instability of the delithiated material.[11]

One of the reasons for the poor performance of the orthosilicates may be their very low intrinsic electronic conductivity, which causes excessive polarisation during charge-discharge cycling. In order to overcome this problem, approaches such as coating the silicate particles with carbon to produce Li_2MnSiO_4–C composites are being pursued.[15–19] It has also been reported that antisite disorder is more prevalent in the Fe analogue than in the Mn analogue,[16] because the ionic radius of Fe is closer to that of Li than Mn, although partial occupancies of about 5 and 10% have been reported for Li on Mn sites in some preparations.[11]

Li_2MSiO_4 (M = Fe, Mn, Co) compounds are known to exhibit a rich polymorphism,[20] and several crystal structures have been reported in the literature.[12,21–26] The archetypal compound is Li_3PO_4, where replacement of one Li with Mn, and P with Si,

[a]*Nanostructures Research Laboratory, Japan Fine Ceramics Center, 2-4-1 Mutsuno, Atsuta-ku, Nagoya, Japan. E-mail: c_fisher@jfcc.or.jp*

[b]*Department of Chemistry, University of Bath, Bath BA2 7AY, UK*

† Electronic supplementary information (ESI) available: Buckingham potential parameters used and bond distance/angle measurements for each polymorph. See DOI: 10.1039/c3ta00111c

‡ Present address: Department of Physics and Astronomy, University College London, Gower Street, London WC1E 6BT, UK.

gives the composition Li_2MnSiO_4. Dominko *et al.*[11] reported their samples of Li_2MnSiO_4 to have an orthorhombic structure (based on β-Li_3PO_4), isostructural with orthorhombic Li_2FeSiO_4 ($Pmn2_1$), and known as the β_{II} phase. Politaev *et al.*[22] reported a monoclinic structure ($P2_1/n$), based on γ-Li_3PO_4 and known as the γ_0 phase, which is similar to that of monoclinic Li_2FeSiO_4 synthesised by Nishimura *et al.*[23] By examining a number of compositions of the solid solution $Li_2(Fe_{1-x}Mn_x)SiO_4$, Sirisopanaporn *et al.*[24] showed that the orthorhombic β_{II} phase is a low temperature polymorph, while the monoclinic γ_0 phase is a high temperature form. A third polymorph which shares features of the other two and has an orthorhombic structure (*Pmnb*) has also recently been characterised,[25] referred to as the γ_{II} phase. Another monoclinic phase with *Pn* symmetry has also recently been synthesised by ion exchange from Na_2MnSiO_4, and is stable up to 370 °C.[26] For both of the non-orthogonal forms, the monoclinic angles deviate only slightly (≤1°) from 90°.

The crystal structures of these four polymorphs are illustrated in Fig. 1. All are based on a distorted hexagonal close-packed array of oxide ions with all cations in distorted corner-sharing tetrahedra, but they differ in the orientation of these tetrahedra, particularly for the MnO_4–SiO_4 chains. The $Pmn2_1$ and *Pn* structures, belonging to non-centrosymmetric space groups, have their MnO_4 and SiO_4 tetrahedra all pointing in the same direction parallel to their *c* axes. In the *Pmnb* and $P2_1/n$ structures, which both belong to centrosymmetric space groups, half the MnO_4 and SiO_4 tetrahedra point in one direction, and the other half in the opposite direction, for each of the three crystal axes. Another key difference is that while in the $Pmn2_1$ and *Pn* phases all tetrahedra are corner-sharing, in the *Pmnb* phase pairs of LiO_4 tetrahedra share an edge, and in the $P2_1/n$ phase each $Li(2)O_4$ tetrahedron shares edges with both an MnO_4 tetrahedron and an $Li(1)O_4$ tetrahedron. Consequently in the orthorhombic phases LiO_4 tetrahedra form distinct sheets sandwiched between MnO_4 and SiO_4 tetrahedral sheets in the [010] plane, while in the monoclinic phases the three types of tetrahedral units are interconnected in all three crystallographic directions.

Atomistic simulation provides a reproducible and systematic means of comparing the inherent stabilities of each polymorph, as well as enabling analysis of defect properties, conductivity mechanisms and other features pertinent to their electrochemical performance at a fundamental level. *Ab initio* methods have already been used by several groups to examine changes in electronic structure and relative phase stabilities of different phases of Li_xMSiO_4 (M = Mn, Fe, Co and Ni) compounds.[21,27–32] In this study we use well-established empirical-potential-based methods to investigate the complex defect energetics and Li-ion migration mechanisms for the four reported polymorphs of Li_2MnSiO_4. This work extends our previous examination of the

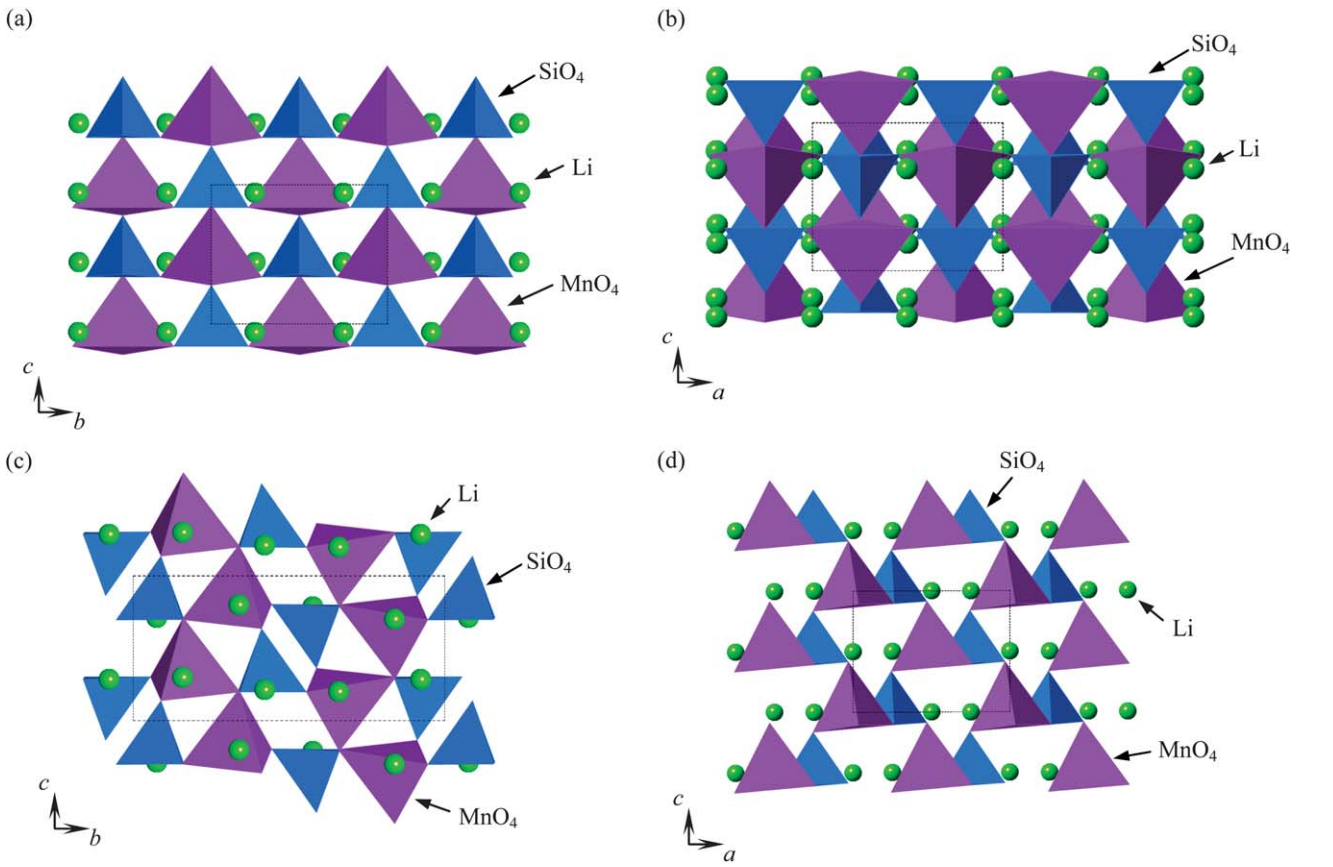

Fig. 1 Crystal structures of Li_2MnSiO_4 polymorphs showing arrangement of MnO_4 (purple) and SiO_4 (blue) tetrahedra, together with Li ions (green): (a) orthorhombic $Pmn2_1$ phase; (b) orthorhombic *Pmnb* phase; (c) monoclinic $P2_1/n$ phase; (d) monoclinic *Pn* phase. Unit cells are indicated by dashed lines.

defect properties and doping behavior of the $Pmn2_1$ and $P2_1/n$ polymorphs,[33] and forms part of a continuing effort to understand the structure–property relationships in lithium-ion battery materials with the aim of promoting development of batteries with superior performance and environmental benignity.

Methodology

The simulation methodologies employed have been applied successfully to a wide range of inorganic solids, including lithium battery materials Li_2FeSiO_4,[34] $LiFeSO_4F$,[35] $LiVO_2$,[36] $Li_2FeP_2O_7$,[37] and olivine phosphates $LiMPO_4$ (M = Fe, Co, Mn, Ni).[38] Detailed reviews are available elsewhere[39,40] so only a brief account will be given here. The cohesive properties of the ideal (defect-free) crystal structure, including physical properties such as elastic and dielectric constants and bulk (Voigt-Reuss-Hill, VRH) modulus, were calculated using energy minimisation techniques. Defect formation and migration energies were subsequently calculated using the Mott–Littleton approach[41] commencing from the optimised crystal geometry. The interatomic potential model used was based on a Born model representation of polar solids, in which forces are assumed to be a function of the distance between particles. Pairwise interactions were divided into long-range Coulombic and short-range components, with the short-range term described by an analytical function of the Buckingham form. A three-body term was also incorporated into the model to take into account the angle-dependent nature and rigidity of silicate bonds within SiO_4 tetrahedra. Electronic polarizability of Mn^{2+} and O^{2-} ions was incorporated using the shell model.[42]

All the parameters used in this study are provided as ESI.† Ion migration calculations were performed within the Mott–Littleton framework by creating two vacancies on neighboring Li sites and systematically placing an Li ion at regular intervals along the diagonal connecting them. In this way, the minimum energy surface crossed by a migrating Li ion could be traced for each possible migration path assuming an ion hop mechanism. All simulations were performed using the code GULP.[43]

Results and discussion

Crystal structures and phase stabilities

The unit cell dimensions and ion positions of each polymorph were equilibrated (relaxed to zero force) under constant pressure conditions commencing from experimentally determined crystal structures reported in the literature. A comparison of the calculated and experimental lattice parameters and volumes is made in Table 1 for the four polymorphs. The lattice parameters for polymorphs $Pmn2_1$, $Pmnb$, and $P2_1/n$ vary by at most 1.9% from the experimentally determined values, with average deviations of around 1%. The deviation from the experimental structure is slightly greater for the *Pn* polymorph at around 3%, but still comparable with results of DFT calculations using GGA(+U) for the exchange-correlation functional.[26] Overall our calculated bond and angle values are in excellent agreement with those calculated from the ideal (non-defective) structures using first-principles DFT methods.[21,26] The reproduction of the monoclinic angles in the $P2_1/n$ and *Pn* polymorphs is particularly good.

Table 1 Comparison between experimental and calculated lattice parameters of four polymorphs of Li_2MnSiO_4

Phase	a (Å)	b (Å)	c (Å)	β (°)
$Pmn2_1$				
Exp.[a]	6.311	5.380	4.966	90.0
Calc.	6.432	5.359	4.910	90.0
Pmnb				
Exp.[b]	6.307	10.754	5.009	90.0
Calc.	6.409	10.734	4.970	90.0
$P2_1$/n				
Exp.[c]	6.336	10.915	5.073	90.987
Calc.	6.428	10.993	5.045	90.891
Pn				
Exp.[d]	6.593	5.402	5.090	89.7
Calc.	6.391	5.540	4.940	89.7

[a] Ref. 11. [b] Ref. 25. [c] Ref. 22. [d] Ref. 26.

Calculated bond distances and angles, provided as ESI,† were also compared with their corresponding experimental values. These too are in excellent agreement, with discrepancies of at most 0.11 Å in the interatomic distances, and angle deviations within at most a few degrees. Given the difficulty in developing transferable, reliable sets of potential parameters, especially for complex structures such as those encountered here, the ability to reproduce the details of all four structures accurately gives us confidence that our model provides a good representation of the underlying physics and chemistry of this system.

Table 2 summarises the calculated properties for each polymorph. Comparison of the lattice energies, LE, shows that the two orthorhombic phases are slightly more stable than the monoclinic phases, consistent with the observed stabilities reported by Sirisopanaporn *et al.*[24] and those obtained from first-principles calculations.[21,32] The difference in lattice energies between the $P2_1$/n and $Pmn2_1$ phases is less than 10 meV, which suggests in practice both phases are equally stable. The least stable phase is calculated to be the *Pn* phase, with an energy difference compared to the $Pmn2_1$ phase of around 100 meV. In addition, calculation of the phonon dispersion curves revealed no soft modes for any of the phases, indicating that all four structures are stable, rather than metastable, at low

Table 2 Comparison of crystal properties (lattice energies, LE; static dielectric constant, ε_0; elastic constants, c; bulk (VRH) modulus, B) of four polymorphs of Li_2MnSiO_4

Property						
Phase	LE (eV)	ε_0	c_{11} (GPa)	c_{22} (GPa)	c_{33} (GPa)	B (GPa)
$Pmn2_1$	−202.80	5.7	277.0	132.7	153.3	106.4
Pmnb	−202.79	5.7	275.3	137.2	148.0	108.6
$P2_1/n$	−202.72	6.0	111.3	189.5	136.7	98.7
Pn	−202.68	6.0	135.4	180.5	145.2	99.0

temperatures. These small differences in lattice energies between the different phases, and hence their similar stabilities, explains the difficulty of preparing single phases of the individual polymorphs. Interestingly, DFT calculations by Kalantarian *et al.*[32] on three of these polymorphs recently demonstrated that this stability order is altered upon delithiation, suggesting a plausible cause for the dramatic changes in structure and degradation of the electrochemical properties typically observed after the first few cycles. We discuss this aspect in more detail in the section on lithium-ion migration.

The data in Table 2 also shows that the *Pmnb* and $Pmn2_1$ phases have very similar physical properties, at least in the case of their static dielectric (ε_0) and principal elastic constants (c_{11}, c_{22} and c_{33}), while the properties of the $P2_1/n$ phase are more similar to those of the *Pn* phase. Although no experimental data on dielectric and elastic properties are available for further validation or refinement of the potential model, the good reproduction of the lattice parameters, atom positions and bond lengths of the four polymorphs suggests that the calculated physical properties are at least of the correct order of magnitude and should reflect the trends in the actual materials. For example, the calculated bulk moduli of the two orthorhombic phases are marginally higher than that of the monoclinic phases, indicating greater rigidity of their structures. This is consistent with results from DFT calculations of Li_2MnSiO_4 and Li_2CoSiO_4 at high pressures,[44] which predict the moduli of the $Pmn2_1$ and *Pmnb* phases to be almost identical, although the DFT-calculated values are closer to those reported from experiment, at least for the $Pmn2_1$ phase.[11]

Intrinsic defects and off-stoichiometry

Energies of isolated point defects (vacancies, interstitials and site exchange) were calculated using a cut-off distance of 12 Å for the inner defect region, corresponding to slightly more than 1000 atoms, and the results combined to give the energies of Frenkel, Schottky and other types of possible disorder modes. These are summarised for each polymorph in Table 3. It should be noted that only lithium, manganese, and oxygen interstitial ions were considered, as the tetravalent silicon ions with their high ionic charges are unlikely to exist isolated from oxygen tetrahedra. The high energies for O Frenkel disorder indicate that excess superoxide states are highly unstable, as expected.

The energies in Table 3 reveal that the predominant mode of intrinsic disorder is cation exchange, *i.e.*, antisite disorder in which an Li^+ ion occupies an Mn^{2+} lattice site, and *vice versa*. This result is consistent with Rietveld refinements of these phases showing that the nominal Li and Mn sites are partially occupied by the other ion.[11] It is also worth noting that, according to computational analyses, antisite defects are the most common intrinsic defect form for olivine-type $LiMPO_4$ (M = Mn, Fe, Co, Ni) compounds;[38] the presence of such defects has recently been confirmed experimentally in the case of the Fe analogue.[45] As this is an endothermic process, the concentration of antisite defects should be temperature dependent and hence sensitive to experimental synthesis conditions.

Another trend evident in the results is that defects are more easily formed in the monoclinic phases compared to the orthorhombic phases. This may be related to the slightly lower rigidity of the structures, as reflected in the lower bulk moduli and elastic constants of the former, which allows them to accommodate local lattice strain without incurring as high an energy penalty.

Our treatment of electronic defects follows that used for other transition metal compounds (*e.g.*, $LiMPO_4$ where M = Mn, Fe, Co, Ni)[13] in which hole ($h^{\cdot}$) species are modelled as a small polaron on manganese (Mn^{3+}) or oxygen (O^{-}). Although in real systems there will be a degree of Mn(3d)–O(2p) mixing, for the purpose of assessing the relative feasibility of different hole formation reactions these methods have proven valuable. Within our model, oxidation by localisation of the hole on an Mn ion (Mn^{3+}) is found to be more energetically favourable than an O^{-} polaron.

Comparison of the off-stoichiometry defect energies in Table 2 shows that Li deficiency occurs slightly more easily as a result of Mn excess rather than through oxidation, although the magnitude of neither process is particularly low. This suggests the materials do not exhibit significant non-stoichiometry and that it should be possible to synthesise materials with close to full lithium content without too much difficulty as long as Li evaporation at elevated temperatures is avoided.

Lithium-ion migration

Each of the polymorphs considered in this study has a relatively complex structure for a solid-state ionic conductor (*cf.* the

Table 3 Comparison of defect energies for four polymorphs of Li_2MnSiO_4

		Energy (eV/defect)			
Disorder type	Defect equation (Kröger–Vink notation)	$Pmn2_1$	*Pmnb*	$P2_1/n$	*Pn*
Li Frenkel	$Li_{Li}^{\times} \rightarrow Li_i^{\cdot} + V_{Li}^{'}$	2.03	1.92	1.27	1.53
Mn Frenkel	$Mn_{Mn}^{\times} \rightarrow Mn_i^{\cdot\cdot} + V_{Mn}^{''}$	3.36	3.27	3.09	3.13
O Frenkel	$O_o^{\times} \rightarrow O_i^{''} + V_o^{\cdot\cdot}$	4.40	4.39	3.85	4.50
Li/Mn antisite	$Li_{Li}^{\times} + Mn_{Mn}^{\times} \rightarrow Mn_{Li}^{\cdot} + Li_{Mn}^{'}$	0.79	0.79	0.67	0.66
Schottky	$2Li_{Li}^{\times} + Mn_{Mn}^{\times} + Si_{Si}^{\times} + 4O_O^{\times} \rightarrow 2V_{Li}^{'} + V_{Mn}^{''} + V_{Si}^{''''} + 4V_O^{\cdot\cdot}$	5.44	5.15	4.82	5.10
Li deficiency (oxidation)	$2Li_{Li}^{\times} + \frac{1}{2}O_2 \rightarrow 2V_{Li}^{'} + 2h^{\cdot} + Li_2O$	2.02	2.01	1.64	1.60
Li deficiency (Mn excess)	$MnO + 2Li_{Li}^{\times} \rightarrow Mn_{Li}^{\cdot} + V_{Li}^{'} + Li_2O$	1.90	1.89	1.53	1.54

rhombohedral structure of $LiCoO_2$), with two or more different Li–Li interatomic distances per unit cell. From the crystal symmetries alone a certain amount of anisotropy can be expected in the Li-ion conductivities of each crystal, as Li-ion migration barriers are known to vary as a function of the Li–Li jump distance and local bonding environment. The most likely migration pathways in each polymorph were identified by connecting the shorter of the Li–Li interatomic distances in each crystal to form continuous pathways.[33] These are illustrated in Fig. 2 in the form of arrows between Li sites; with Roman and Arabic numerals indicating different Li–Li interatomic distances.

Comparison of the structures in Fig. 2 reveals that the orthorhombic $Pmn2_1$ phase provides the simplest migration pathway for an Li ion, since it has the highest symmetry and, because all Li sites in the unit cell are symmetrically equivalent, only one jump distance for each direction (3.1 Å for net [001] migration, and 3.2 Å for net [100] migration). The next simplest migration network is found in the *Pmnb* phase, which although of lower symmetry than the $Pmn2_1$ phase still only has one type of Li site. In both these cases, pathways are available parallel to the *a* and *c* axes; jumps between sites in the *b* direction, however, are energetically unfeasible because of the large Li–Li distances which span interleaving SiO_4 and MnO_4 tetrahedral layers. In the $P2_1/n$ phase, in contrast, there are two symmetrically distinct Li sites, whose vacancy formation energies are slightly different, resulting in a more complex migration network. In this case, contiguous pathways exist in the *b* and *c* directions, with jump distances between 2.7 and 3.5 Å, although the pathway is rather tortuous. We note that these differences in pathways are consistent with the prediction by Kalantarian *et al.*[32] based on a visual assessment of delithiated structures calculated using DFT, although the magnitude of the changes in activation energies turn out perhaps to be not as large as they had envisaged.

Nevertheless, even the small changes in migration barriers can have a large effect on the lithiation/delithiation kinetics. For example, upon transformation of $Pmn2_1$ to $P2_1/n$ (assuming no alteration in the number of charge carriers), a drop of at least 20% can be expected based simply on the ratio of exponential terms in the Arrhenius equation governing ion migration. In practice, the particular changes that occur will depend on the synthesis method and conditions, but drops in capacity of around 50% after the first couple of cycles are typically observed.[11,17] Based on early observations that certain synthesis strategies can lead to amorphisation during cycling, it is likely that large numbers of antisite defects also accompany the phase transformation during removal and insertion of Li, even when the structure remains crystalline; this also undoubtedly contributes significantly to the drop in capacity because such defects will have a strong blocking effect on particular conduction pathways.

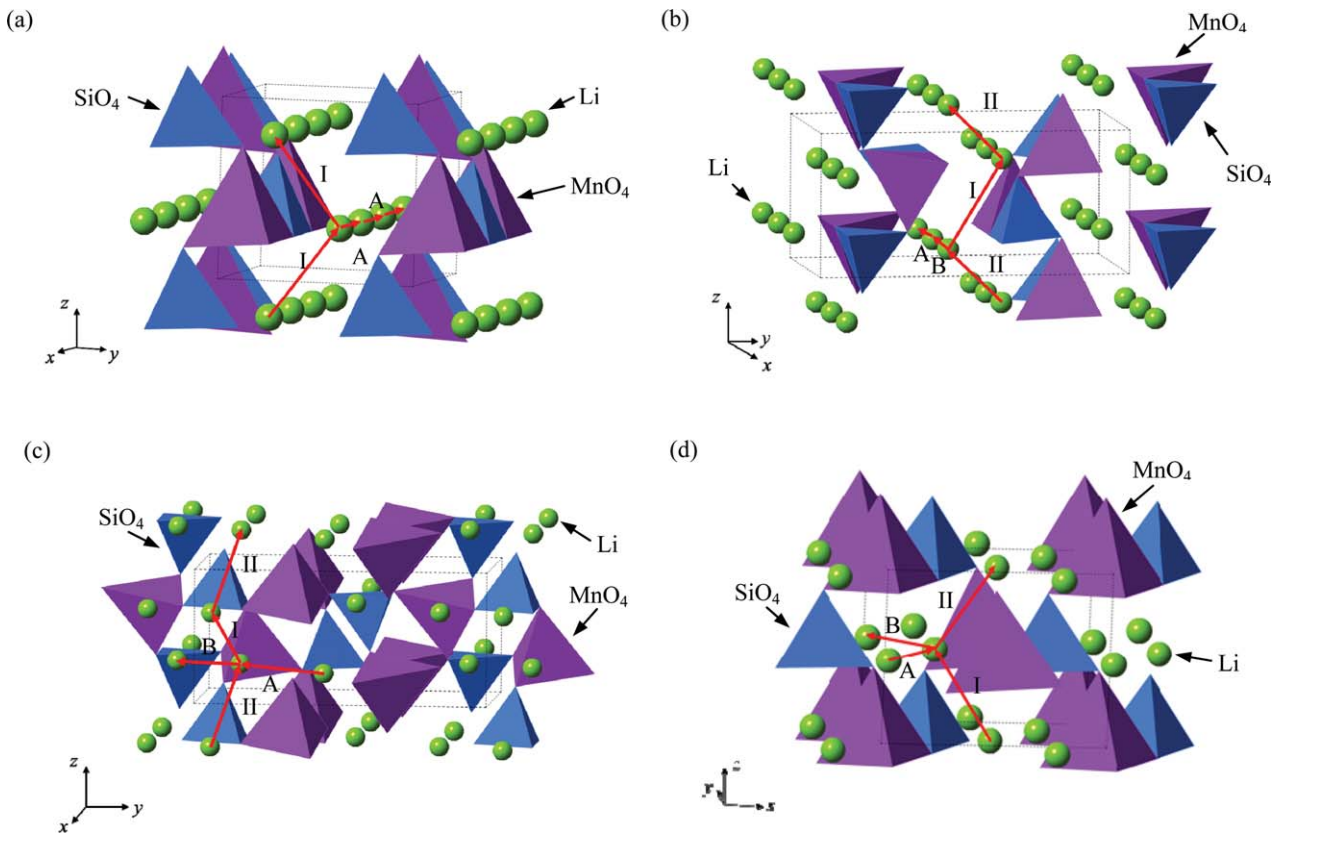

Fig. 2 Li-ion migration pathways in Li_2MnSiO_4 polymorphs with respect to MnO_4 and SiO_4 tetrahedra: (a) orthorhombic $Pmn2_1$ phase; (b) orthorhombic *Pmnb* phase; (c) monoclinic $P2_1/n$ phase; and (d) monoclinic *Pn* phase. Unit cells are indicated by dashed lines.

In the case of the *Pn* phase, migration is feasible along zigzag pathways in the [100] and [001] directions, although the intersite jump distances are large at 3.0 to 3.4 Å. For the orthorhombic phases, Li conduction is expected to be two-dimensional, although it is possible a certain concentration of antisite defects may provide alternative pathways, albeit with high activation barriers. In contrast, three-dimensional conductivity is possible in the monoclinic phases, although in both cases migration in one of the crystallographic directions can only occur by following a tortuous route involving multiple jumps shared with pathways oriented primarily in one of the other crystallographic directions.

Calculated energy profiles for isolated Li^+ ions migrating by a hopping mechanism between pairs of lattice vacancies, corresponding to each of the migration paths in Fig. 2, are shown in Fig. 3. Note that the horizontal axes indicate the distance along the trajectory of the migrating ion for the two simplest migration pathways in each crystal, which are curved rather than straight. As reported earlier for the *Pmnb* and $Pmn2_1$ polymorphs, even the shortest jumps require high activation energies to be overcome in order for long-range Li-ion migration to occur. The highest energy barriers for these paths are listed in Table 4 for each polymorph. For the $Pmn2_1$ phase, activation energies are similar in both the *a* and *c* directions at slightly over 1 eV. In the case of the *Pmnb* phase, energy barriers are less uniform in the [001] direction, varying from 0.6 to 1.4 eV, while in the [100] direction they are similar to the $Pmn2_1$ phase at around 1 eV. A similar variation in barrier energies for hops in the monoclinic $P2_1/n$ phase occurs, with a low of 0.3 eV for one

Table 4 Calculated activation energies for Li-ion migration in four polymorphs of Li_2MnSiO_4. Numbers in parentheses are the jump distances in angstroms

Activation energy (eV)				
	Direction			
Phase	A	B	I	II
$Pmn2_1$	1.13 (3.22)	—	1.03 (3.07)	—
Pmnb	1.08 (3.19)	1.05 (3.22)	1.36 (3.62)	0.58 (2.57)
$P2_1/n$	1.40 (3.50)	0.32 (2.91)	0.62 (2.67)	0.92 (3.49)
Pn	0.65 (2.90)	1.72 (4.34)	1.02 (3.05)	1.00 (3.44)

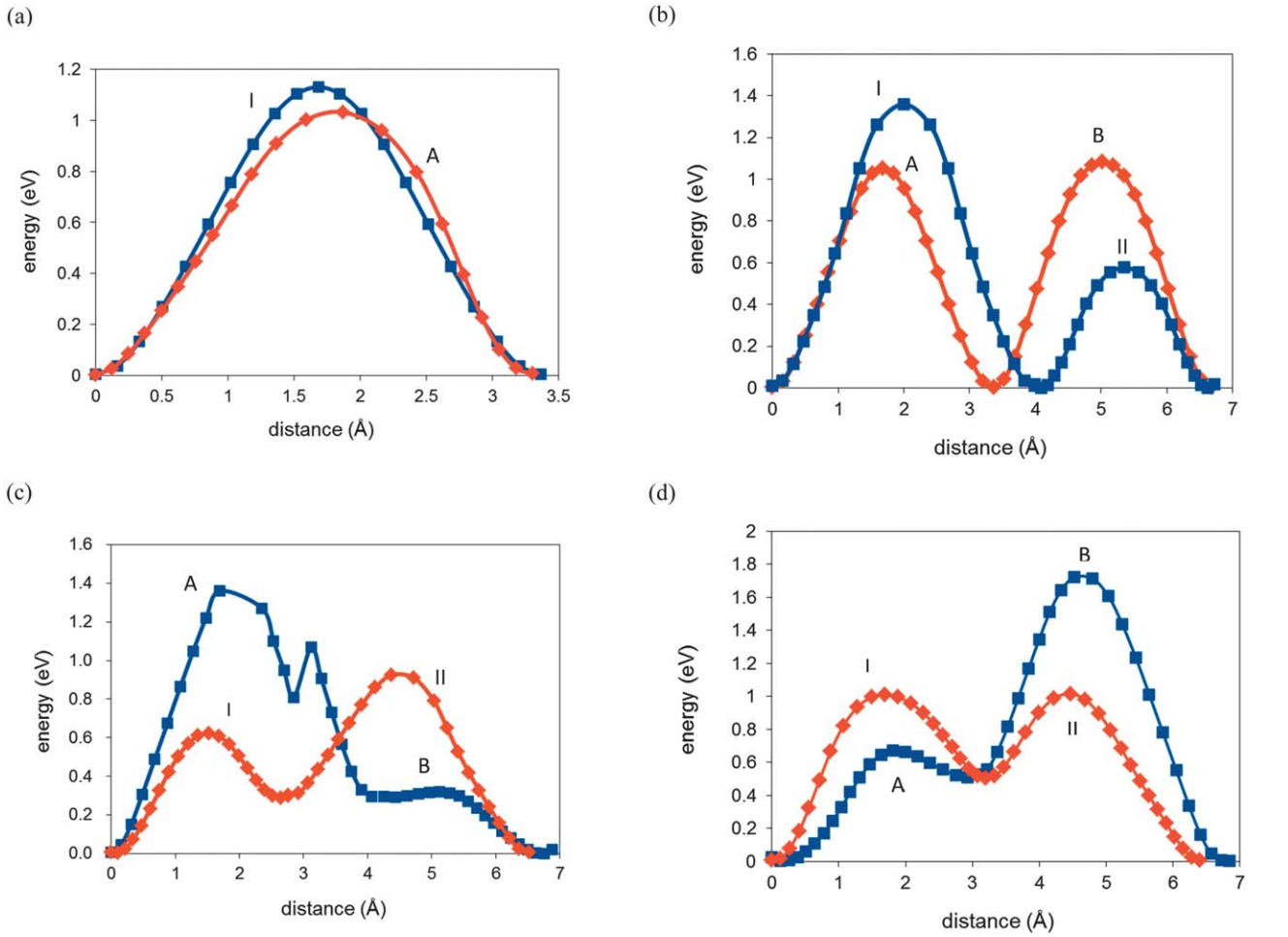

Fig. 3 Energy profiles encountered by single Li^+ ions migrating by vacancy hopping for the two lowest energy pathways within each Li_2MnSiO_4 polymorph: (a) orthorhombic $Pmn2_1$ phase; (b) orthorhombic *Pmnb* phase; (c) monoclinic $P2_1/n$ phase; and (d) monoclinic *Pn* phase. Note that the horizontal axes indicate the distance along the trajectory of the migrating ion for the two simplest migration pathways in each crystal, which are curved rather than straight.

hop increasing to about 1.4 eV for the connecting hop in the [010] direction, and 0.6 eV and 0.9 eV in the [001] direction. Strong anisotropy in the *Pn* phase is also evident, with the activation energy in the [100] direction almost twice that in the [001] direction. Overall the results suggest that Li-ion diffusion coefficients and hence Li-ion conductivities are lowest for the orthorhombic $Pmn2_1$ phase. Altogether the results indicate that all four polymorphs are poor Li conductors (at room temperature), in good agreement with experimental reports that the materials need to be prepared as nanoparticles[15,18,46] or nanofibres[47] before they become electrochemically active.

As mentioned earlier, detailed analysis of the trajectories of migrating Li ions in each polymorph shows that, rather than direct linear paths, the ions follow curved pathways between Li sites in response to the asymmetry in the local coordination environments. Similar curved pathways have been predicted in many other inorganic ion conductors, such as Sr- and Mg-doped $LaGaO_3$ (ref. 48) and $LiMPO_4$ (M = Mn, Fe, Co, Ni),[38] using computer simulation, which were later confirmed using a combination of Rietveld refinement and maximum-entropy-method-based pattern fitting.[49,50] In Li_2MnSiO_4, these deviations from a simple linear path are typically within 0.2 Å, but as a result of the complexity of their crystal structures are less uniform than in perovskite- or olivine-structured compounds.

Conclusions

This systematic survey of four polymorphs of Li_2MnSiO_4 using atomistic simulation techniques provides detailed insights into defect and lithium ion-migration properties relevant to their electrochemical behaviour. The main results can be summarised as follows:

(1) The two orthorhombic phases ($Pmn2_1$, *Pmnb*) have very similar dielectric and elastic constants, as well as bulk moduli, while the properties of the two monoclinic phases ($P2_1/n$ and *Pn*) are also similar to one another.

(2) The observed crystal structures of all four phases were successfully reproduced by our potential model, with excellent agreement between calculated bond distances and angles and those from experiment where this was possible. The most favourable intrinsic defect in all four cases is the antisite defect; a small population of Li^+ and Mn^{2+} ions is thus expected to exchange sites, in good agreement with the partial cation occupancies typically reported for these materials.

(3) Deviation from stoichiometry is most easily achieved by the presence of Mn on Li sites (Mn excess) for all phases. The intermediate energies required to form Li-poor compositions suggests stoichiometric samples of this compound should be possible under suitable conditions.

(4) Detailed analysis of the Li-ion hopping mechanism shows that lithium ions follow tortuous migration paths, with jump distances varying significantly in at least one crystallographic direction of each polymorph, from 2.6 to 3.6 Å. For each hop between two vacant lattice sites, Li ions follow curved trajectories similar to those observed in other Li-ion conductors such as $LiFePO_4$. All four polymorphs are predicted to be poor Li-ion conductors at room temperature on account of their high activation energies (at least 1 eV), which implies low rate capabilities for Li_2MnSiO_4-based cathodes unless synthesised as nanoparticles to facilitate rapid Li transfer. The two orthorhombic phases are predicted to display essentially two-dimensional Li-ion conductivity, while the monoclinic phases should exhibit three-dimensional ion conductivity, but with strong anisotropy.

(5) The lowest migration energy barrier is found for the orthorhombic $Pmn2_1$ phase. Based on a simple comparison of the kinetics of lithium extraction/insertion, the phase changes during initial cycling are expected to lead to a sharp loss in capacity, as is observed experimentally. This is expected to be further exacerbated by the ease of formation of Li/Mn antisite defects, which will impede Li-ion migration.

Acknowledgements

The authors thank Dr R. J. Gummow of James Cook University and Dr A. R. Armstrong of the University of St Andrews for helpful discussions. N. K. thanks the UK's EPSRC Supergen programme for financial support.

References

1 M. Armand and J.-M. Tarascon, *Nature*, 2008, **451**, 652; V. Etacheri, R. Marom, R. Elazari, G. Salitra and D. Aurbach, *Energy Environ. Sci.*, 2011, **4**, 3243; B. L. Ellis, K. T. Lee and L. F. Nazar, *Chem. Mater.*, 2010, **22**, 691.
2 M. M. Thackeray, P. J. Johnson, L. A. de Picciotto, P. G. Bruce and J. B. Goodenough, *Mater. Res. Bull.*, 1984, **19**, 179.
3 Y. K. Yoon, C. W. Park, H. Y. Ahn, D. H. Kim, Y. S. Lee and J. Kim, *J. Phys. Chem. Solids*, 2007, **68**, 780; M. Okubo, Y. Mizuno, H. Yamada, J. Kim, E. Hosono, H. Zhou, T. Kudo and I. Honma, *ACS Nano*, 2010, **4**, 741; R. Singhal, J. J. Saavedra-Aries, R. Katiyar, Y. Ishikawa, M. J. Vilkas, S. R. Das, M. S. Tomar and R. S. Katiyar, *J. Renewable Sustainable Energy*, 2009, **1**, 023102.
4 C. S. Johnson, N. Li, C. Lefief and M. M. Thackeray, *Electrochem. Commun.*, 2007, **9**, 787; D. Y. W. Yu and K. Yanagida, *J. Electrochem. Soc.*, 2011, **158**, A1015.
5 J. Wilcox, S. Patoux and M. Doeff, *J. Electrochem. Soc.*, 2009, **156**, A192.
6 A. K. Padhi, K. S. Nanjundaswamy and J. B. Goodenough, *J. Electrochem. Soc.*, 1997, **144**, 1188.
7 M. S. Whittingham, Y. Song, S. Lutta, P. Y. Zavalij and N. A. Chernova, *J. Mater. Chem.*, 2005, **15**, 3362.
8 J. Barker, R. K. B. Gover, P. Burns and A. Bryan, *J. Electrochem. Soc.*, 2007, **154**, A307.
9 J. Gaubicher, C. Wurm, G. Goward, C. Masquelier and L. Nazar, *Chem. Mater.*, 2000, **12**, 3240.
10 A. Nytén, A. Abouimrane, M. Armand, T. Gustaffson and J. O. Thomas, *Electrochem. Commun.*, 2005, **7**, 156; A. Nytén, S. Kamali, L. Häggström, T. Gustaffson and J. O. Thomas, *J. Mater. Chem.*, 2006, **16**, 2266.
11 R. Dominko, M. Bele, M. Gaberščček, A. Meden, M. Remškar and J. Jamnik, *Electrochem. Commun.*, 2006, **8**, 217;

R. Dominko, M. Bele, A. Kokalj, M. Gaberscek and J. Jamnik, *J. Power Sources*, 2007, **174**, 457.
12 C. Lyness, B. Delobel, A. R. Armstrong and P. G. Bruce, *Chem. Commun.*, 2007, 4890.
13 A. Nyten, A. Abouimrane, M. Armand, T. Gustafsson and J. O. Thomas, *Electrochem. Commun.*, 2005, **7**, 156.
14 C. Sirisopanaporn, A. Boulineau, D. Hanzel, R. Dominko, A. R. Armstrong, P. G. Bruce and C. Masquelier, *Inorg. Chem.*, 2010, **49**, 7446.
15 Z. L. Gong, Y. X. Li and Y. Yang, *Electrochem. Solid-State Lett.*, 2006, **9**, A542; Y.-X. Li, Z.-L. Gong and Y. Yang, *J. Power Sources*, 2007, **174**, 528.
16 X. Huang, X. Li, H. Wang, Z. Pan, M. Qu and Z. Yu, *Solid State Ionics*, 2010, **181**, 1451.
17 V. Aravindan, K. Karthikeyan, J. W. Lee, S. Madhavi and Y. S. Lee, *J. Phys. D: Appl. Phys.*, 2011, **44**, 152001.
18 I. Belharouak, A. Abouimrane and K. Amine, *J. Phys. Chem. C*, 2009, **113**, 20733; Q. Zhang, Q. Zhuang, S. Xu, X. Qiu, Y. Cui, Y. Shi and Y. Qiang, *Ionics*, 2012, **18**, 487.
19 V. Aravindan, K. Karthikeyan, K. S. Kang, W. S. Yoon, W. S. Kim and Y. S. Lee, *J. Mater. Chem.*, 2011, **21**, 2470.
20 M. S. Islam, R. Dominko, C. Masquelier, C. Sirisopanaporn, A. R. Armstrong and P. G. Bruce, *J. Mater. Chem.*, 2011, **21**, 9811.
21 M. E. Arroyo-deDompablo, M. Armand, J. M. Tarascon and U. Amador, *Electrochem. Commun.*, 2006, **8**, 1292; M. E. Arroyo-deDompablo, R. Dominko, J. M. Gallardo-Amores, L. Dupont, G. Mali, H. Ehrenberg, J. Jamnik and E. Morán, *Chem. Mater.*, 2008, **20**, 5574.
22 V. V. Politaev, A. A. Petrenko, V. B. Nalbandyan, B. S. Medvedev and E. S. Shvetsova, *J. Solid State Chem.*, 2007, **180**, 1045.
23 S. Nishimura, S. Hayase, R. Kanno, M. Yashima, N. Nakayama and A. Yamada, *J. Am. Chem. Soc.*, 2008, **130**, 13212.
24 C. Sirisopanaporn, R. Dominko, C. Masquelier, A. R. Armstrong, G. Maliad and P. G. Bruce, *J. Mater. Chem.*, 2011, **21**, 17823.
25 R. J. Gummow, N. Sharma, V. K. Peterson and Y. He, *J. Solid State Chem.*, 2012, **188**, 32.
26 H. Duncan, A. Kondamreddy, P. H. J. Mercier, Y. Le Page, Y. Abu-Lebdeh, M. Couillard, P. S. Whifield and I. J. Davidson, *Chem. Mater.*, 2011, **23**, 5446.
27 P. Larsson, R. Ahuja, A. Nytén and J. O. Thomas, *Electrochem. Commun.*, 2006, **8**, 797.
28 G. Zhong, Y. Li, P. Yan, Z. Liu, M. Xie and H. Lin, *J. Phys. Chem. C*, 2010, **114**, 3693.
29 G. Mali, A. Meden and R. Dominko, *Chem. Commun.*, 2010, **46**, 3306.
30 C. Eames, A. R. Armstrong, P. G. Bruce and M. S. Islam, *Chem. Mater.*, 2012, **24**, 2155.
31 S. Q. Wu, Z. Z. Zhu, Y. Yang and Z. F. Hou, *Comput. Mater. Sci.*, 2009, **44**, 1243.
32 M. M. Kalantarian, S. Asgari and P. Mustarelli, *J. Mater. Chem. A*, 2013, **1**, 2847.
33 N. Kuganathan and M. S. Islam, *Chem. Mater.*, 2009, **21**, 5196.
34 A. R. Armstrong, C. Lyness, P. Panchmatia, M. S. Islam and P. G. Bruce, *Nat. Mater.*, 2011, **10**, 223.
35 A. R. Armstrong, N. Kuganathan, M. S. Islam and P. G. Bruce, *J. Am. Chem. Soc.*, 2011, **133**, 13031.
36 R. Tripathi, G. R. Gardiner, M. S. Islam and L. F. Nazar, *Chem. Mater.*, 2011, **23**, 2278.
37 J. M. Clark, S. Nishimura, A. Yamada and M. S. Islam, *Angew. Chem., Int. Ed.*, 2012, **51**, 13149.
38 M. S. Islam, D. J. Driscoll, C. A. J. Fisher and P. R. Slater, *Chem. Mater.*, 2005, **17**, 5085; C. A. J. Fisher, V. M. Hart Prieto and M. S. Islam, *Chem. Mater.*, 2008, **20**, 5907.
39 J. H. Harding, *Rep. Prog. Phys.*, 1990, **53**, 1403.
40 M. S. Islam, *Philos. Trans. R. Soc., A*, 2010, **368**, 3255.
41 C. R. A. Catlow, *J. Chem. Soc., Faraday Trans. 2*, 1989, **85**, 335.
42 B. G. Dick and A. W. Overhauser, *Phys. Rev.*, 1958, **112**, 90.
43 J. D. Gale and A. L. Rohl, *Mol. Simul.*, 2003, **29**, 291.
44 D. Santamaría-Pérez, U. Amador, J. Tortajada, R. Dominko and M. E. Arroyo-deDompablo, *Inorg. Chem.*, 2012, **51**, 5779.
45 S.-Y. Chung, Y.-M. Kim and S.-Y. Choi, *Adv. Funct. Mater.*, 2010, **20**, 4219.
46 D. M. Kempaiah, D. Rangappa and I. Honma, *Chem. Commun.*, 2012, **48**, 2698.
47 S. Zhang, Z. Lin, L. Ji, Y. Li, G. Xu, L. Xue, S. Li, Y. Lu, O. Toprakci and X. Zhang, *J. Mater. Chem.*, 2012, **22**, 14661.
48 M. S. Khan, M. S. Islam and D. Bates, *J. Phys. Chem. B*, 1998, **102**, 3099.
49 M. Yashima, K. Nomura, H. Kageyama, Y. Miyazaki, N. Chitose and K. Adachi, *Chem. Phys. Lett.*, 2003, **380**, 391.
50 S. Nishimura, G. Kobayashi, K. Ohoyama, R. Kanno, M. Yashima and A. Yamada, *Nat. Mater.*, 2008, **7**, 707.

